

LIGHTNING RESPONSE OF A COMPOSITE WING TEST BOX: A VALIDATION OF SIMULATION RESULTS

C. Weber*, D. Lalonde †, W. Tse †, S. Brault †, F. Ahmad †, J. Kitaygorsky*

* Electromagnetic Applications Inc., USA, cody@ema3d.com, † Bombardier, Canada, david.lalonde@aero.bombardier.com

Keywords: Aircraft, Lightning, Fuel Tank, Validation, Computational Electromagnetics

1 Abstract

Currents with lightning waveforms were injected onto an aircraft wing test box comprising of carbon fiber reinforced polymer (CFRP) skins and spars. Computational electromagnetic (CEM) simulation results obtained with EMA3D, a finite difference time domain (FDTD) full wave solver, were compared with experimental data to validate analytical methods used as part of a certification program. An extensive measurement program was completed prior to the wing test box experiments in order to develop simulation techniques and establish material parameters applicable to complex CFRP skins covered with multiple expanded copper foils when interacting with lightning currents. Excellent correlation in wave shape and transient peak values is demonstrated for the majority of current and voltage comparisons providing confidence in a numerical approach to accurately characterize a complex aircraft system's response to lightning.

2 Introduction

The certification requirements of §25.981 necessitate a level of understanding of physical phenomena during a lightning attachment that is challenging to obtain with testing alone. The most critical sources of ignition are excessive currents that heat structural elements to the point of spallation and generate excessive voltages that lead to sparking and dielectric breakdown. To overcome these limitations and certify the design, developing a validated CEM model has become an accepted approach in recent §25.981 certification programs. Numerical simulation is increasingly used to evaluate the lightning response of aircraft structures and systems [1, 2]. CEM analysis can be used to establish expected transient levels for internal arcing or sparking as well as determine the actual transient levels (ATLs) on vehicle wiring [3].

Simulation models can help identify possible design problems and provide critical inputs for certification coupon testing. However, all simulation techniques and methodology must be validated against experimental results for the analysis to support a certification program. A sample flowchart outlining essential steps for using CEM analysis as part of a certification program is displayed in Figure 1.

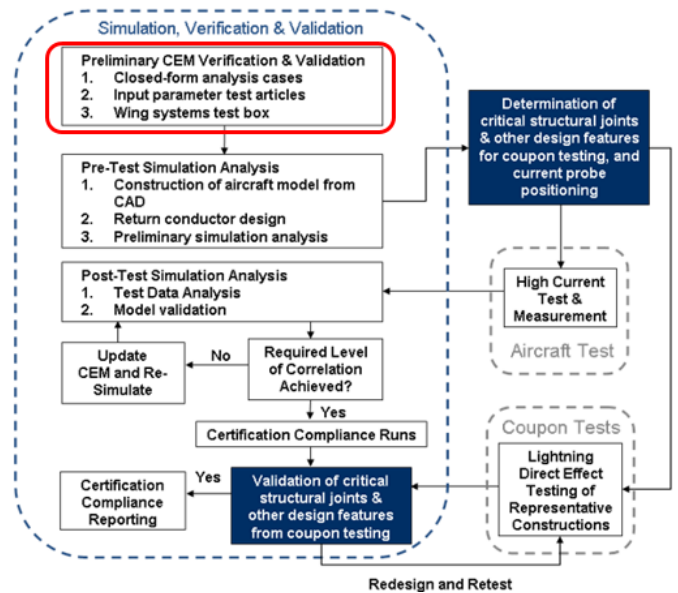


Figure 1. Flowchart illustrating how CEM analysis is used to support an aircraft certification program

This paper focuses on some of the preliminary, but essential steps to developing a certification worthy simulation model as outlined within the red circle of Figure 1. The experimental setup is described along with some of the critical simulation techniques determined to accurately predict all lightning current distribution behaviour for the test box with CFRP skins.

3 Test Box Experimental Setup

The wing test box is a representative section of an aircraft wing, shown in Figure 2, consisting of 5 rib bays. The test box was built by Bombardier with production type materials and construction methods. The dimensions are approximately 2.5 m long, 1m wide and 25 cm in height. The curvature typical to wing skins is excluded from the test article and the overall shape is simplified to be rectangular. CFRP materials were used for the skin panels with multiple types of ECF applied to the upper and lower skins. Access panels are included in the lower skin between each rib bay, typical of aircraft design. The spars are also CFRP but ribs, leading edge structure and trailing edge strap are aluminium. Two separate bundles, 5 wires apiece, are routed separately within the test box. A hydraulic pipe is routed through the center of the tank.

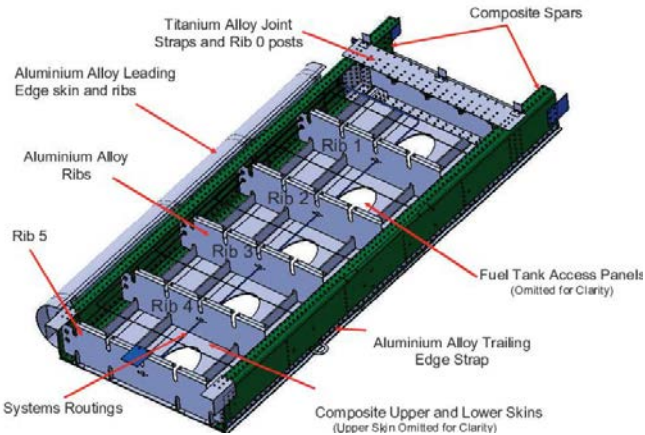


Figure 2: Composite wing test box article illustration.

The experimentally measured quantities were comprised of currents and voltages. Currents were measured on external components such as attach braids, exposed TE spar sections and the TE strap. A significant number of internal currents were measured to fully analyze current flow behavior internal to a composite structured box. These internal current measurements included rib posts, rib sections, wires, hydraulic pipe, LE spar sections and stringer clips. Voltages measured were those that developed between internal wiring and ribs.

The lightning waveform currents were injected at a particular location on the test box and returned through a return conductor system (RCS) built around the test box back to ground. The RCS, as illustrated in Figure 3 and described in [4], was built in order to negate the facility effects and emulate the natural response of the test article.

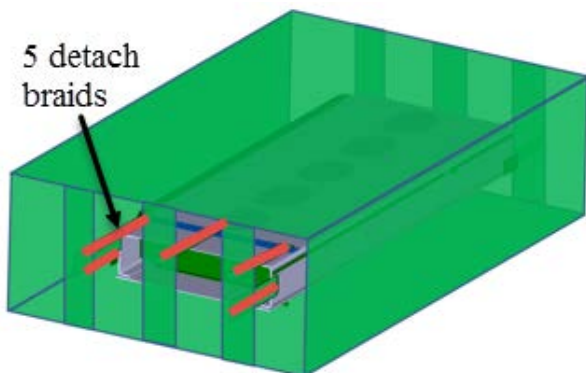


Figure 3: Experimental setup with wing test box article inside of current return network. The 5 detach braid locations are identified in red at the test box root end.

The four strike configurations are described in Table 1. The distributed attachments and detachments at the ends of the test box use metal braids to connect at the LE, center and TE sides and limit the concentration of current to a single location as illustrated in Figure 3. Two fastener injection cases and two cases where current is conducted across the ends of the box were examined. Low level currents similar to the SAE standard component A wave shape [5] were injected

into the test box for all cases. Magnitudes for the injected currents ranged from 2.6 – 10.4 kA with peak times varying from 2.6 – 13.7 μ s.

Table 1. Lightning Current Attachment Cases

Attach location	Detach location
Rib 2 Skin Fastener near box center	Box root – distributed over 5 locations
Rib 3 Skin Fastener near LE side	Box root – distributed over 5 locations
Rib 5 end LE side	Box root – TE side
Rib 5 end – distributed over 3 Locations	Box root – distributed over 5 locations

4 Simulation Approach

The wing test box simulations were executed using EMA3D with integrated MHARNES, a FDTD full wave solver with an integrated transmission line solver. As described in Figure 1, closed form analysis cases were completed using the simulation software to verify its applicability to the transient type EM problem of lightning interaction. The test box numerical model contained significant detail and complexity using a 20 mm cubic cell size. Some of the modelling techniques required to capture an accurate lightning response of a complex CFRP test box system are described below.

It is commonly believed that resolving all anisotropies of ECF and CFRP materials is essential to determining the lightning response of complex systems. There are some limitations to numerical modelling that prohibit the use of anisotropic material definitions for large components with complex curvatures and orientations relative to the principle coordinate axes of the problem space. The effect of using isotropic material properties in place of anisotropic properties has been numerically investigated using two types of wing test box models. The first model resolves the anisotropic behavior of the skins and the second model uses bulk isotropic material definitions for the skins. The simulation results demonstrate that bulk, isotropic material properties in a FDTD simulation can effectively represent an anisotropic configuration.

4.1 Material Property Measurement Program

Aircraft are increasingly utilizing the weight and maintenance benefits provided by CFRP materials. However, CFRP panels are typically 1,000 times less conductive than traditional aluminium materials. It was identified early in the program that fully understanding how CFRP materials with reduced conductivities would interact with lightning currents was an essential step to creating certification worthy numerical models. An additional consideration for aircraft designed using CFRP materials is the electrical connectivity or the resistance between components. The manufacturing processes of composite panels can limit the connectivity of the conductive carbon layers from connecting structures. The electrical connectivity between components is therefore controlled through the joining fasteners. Installation methods

and fastener types can significantly affect the contact resistance of those fasteners, especially when applying a type of sealant or wet installing fasteners.

An essential step to using CEM simulations as part of a certification program is to quantify all material properties and interfaces in the presence of lightning transients. An extensive parameter measurement program took place before the wing test box work to characterize the CFRP and ECF anisotropic material properties. Measurements on numerous samples were also made to determine the contact resistances that existed between production type fasteners and the various structural materials including aluminium structures, ECF, and CFRP panels.

As a verification process for the contact resistance values measured in the program described above, joint resistances of the actual wing test box were measured at DC current levels during different build stages of the test article. An excellent correlation was found between the contact resistance parameters measured with low level lightning transient injections and the resistances of the test box joints using a micro-ohmmeter.

4.2 Bulk Modelling of CFRP Panels with ECF

The mixed carbon ply orientations in the CFRP panel create a decent semi-isotropic conductivity in the planar directions but joining resins create a high resistance in the normal direction. It has been demonstrated that a reduced number of anisotropic simulation layers can be used to capture the flow patterns of multiple layered panels [6]. It is not possible to resolve each layer of the composite panel layup including ECF using a 20 mm mesh size. Therefore, an individual surface in the FDTD model is used to represent the stack of layers in the panel construction.

Many fasteners are used to join the composite panels to structural components like spars and ribs with decent electrical connectivity. The many parallel current paths existing through the penetrating fasteners allow the otherwise isolated panel layers to be treated as a parallel network of conductors. The reduction of a many layered panel into a single FDTD surface representation is illustrated in Figure 4. The characterization of CFRP and ECF material properties allowed the impact of each layer on the bulk conductivity to be understood and quantified. For this bulk representation, the panels connect to the underlying structural components through the fasteners.

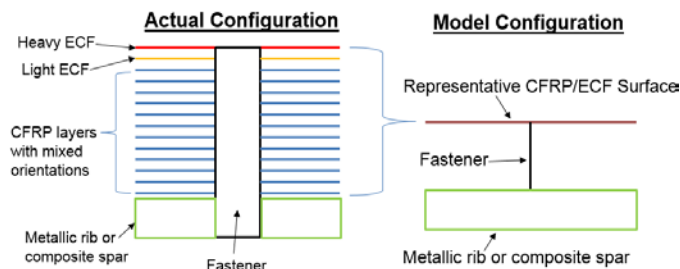


Figure 4: Modelling approach for CRFP panels with ECF.

4.3 Isotropic and Anisotropic Material Properties

The wing test box has a simplified, flat rectangular shape and is aligned with the principle coordinate axes in the FDTD problem space. This type of model can be developed without any stair casing of cells in multiple coordinate directions and lies in a 2D plane. Anisotropic material properties are defined based on a 9x9 conductivity tensor [7] as shown in equation (1).

$$\underline{\underline{\sigma}} = \begin{pmatrix} \sigma_{11} & \sigma_{12} & \sigma_{13} \\ \sigma_{21} & \sigma_{22} & \sigma_{23} \\ \sigma_{31} & \sigma_{32} & \sigma_{33} \end{pmatrix}, \quad \sigma_{ij} \geq 0 \quad (1)$$

In the case of the wing test box, the anisotropic material property can be easily defined for the planar skins. It can be difficult to apply the anisotropic material properties to full aircraft models. Since the numerical modelling approaches will ultimately be applied to a full aircraft certification model, a model using isotropic materials is also needed for the complex wings. Therefore, the wing test box model was simulated using two different skin representations, one with anisotropic bulk conductivities and one with isotropic bulk conductivities, to verify the applicability of the modelling approach to a full scale aircraft.

4.4 Fastener Representation

The fastener contact resistances are a critical model input to capturing distributed lightning current paths through fastened joints in the wing test box. As shown in Figure 5, fasteners can contact multiple material types when joining structures. This can include ECF, multiple CFRP layers and metallic interior structures. The contact resistance value between the fasteners and each material type is typically different, sometimes by more than an order of magnitude. Further complicating the resistance characterization is the fact that contact resistances will vary between fasteners for a particular material. Many samples of materials were tested as described in section 4.1 to determine averaged fastener contact resistances for various material types. While the contact resistance of each individual fastener will vary, the averaged value of fastener contact resistances for a particular material type was used. For structural joints involving many fasteners, it is assumed the total resistance of the joint is the parallel combination of resistors using the averaged fastener contact resistance for a particular material type.

As shown in Figure 5, there are a series of resistances that need to be considered for the connection of two different materials. The contact resistance to material 1, the resistance of the fastener and the contact resistance to material 2 all factor in to the total resistance between two materials. The resistance of the fastener is typically significantly less than either contact resistance and can be neglected from the bulk resistance calculation.

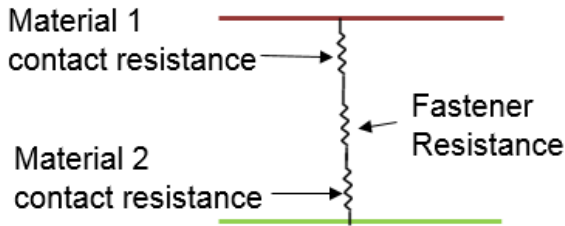


Figure 5: Series of resistances for a fastener connecting two materials.

There are multiple ways to represent a fastener connection within EMA3D models but the contribution from every fastener is considered in the material property specification. In some cases, a single line (1 finite difference cell) is used to represent a single fastener in the model. For other cases, homogenized joints can be used to represent the parallel combination of fastener resistance in a given area as shown in figure 6. For many of the structural connections, actual test box geometries must be modified in the model to include fastened joint representations.

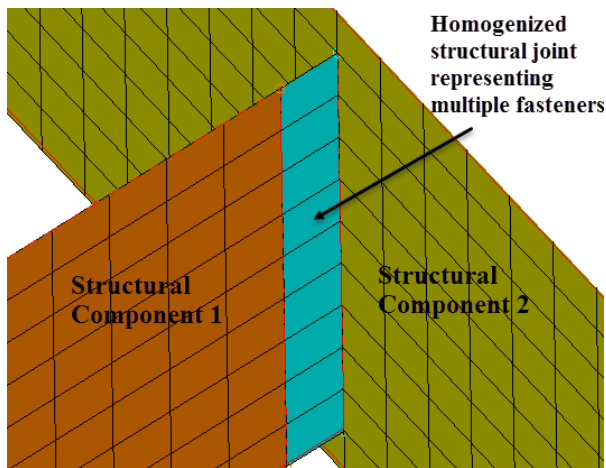


Figure 6: Homogenized joint representation

4.5 Struck Fastener Modelling

The homogenized fastener resistance specification in the previous section works well for joints away from a lightning injection location. However, when trying to predict the amount of injected current that will flow down a struck fastener and onto an interior structure, additional modeling techniques may be required. The injected current can flow onto the skin or through the fastener to the structure beneath. Certain tuning methods can be applied in the model to match experimental results with great precision. As shown in Figure 7, additional resistances can be added to the skin surface to adjust the connectivity of fasteners to exterior skins and interior structures. The exact values to use for the additional surface resistors can be difficult to estimate before experimentation. However, a conservative modeling approach using a relatively low struck fastener resistance or relatively high surface resistor values can be used to determine severe currents flowing onto a rib.

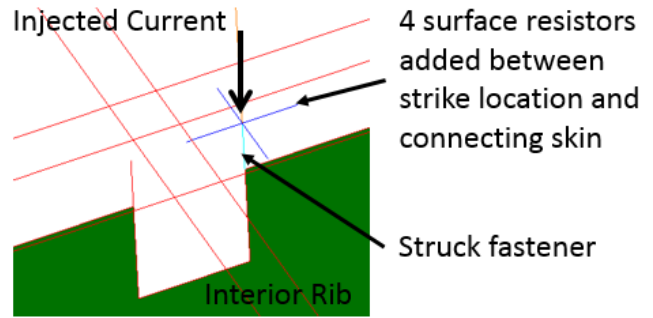


Figure 7: Modelling technique with additional surface resistances for struck fasteners.

4.6 Harness Modelling

The wire harness bundles were modelled using the integrated transmission line solver, MHARNES. This feature allows the discretization and connectivity of individual conductors in a bundle to be resolved within the FDTD problem space. The routing and spatial positioning of each wire in the model accurately reflect the construction of the wing test box and is illustrated in Figure 8. Termination resistances for the wires connecting to structure are also considered in the MHARNES definition. One of the bundles was routed near the upper skin and connected to ribs at the TE side of the test box. The other wire bundle was routed midway between the upper and lower skins and terminated at the rib centers.

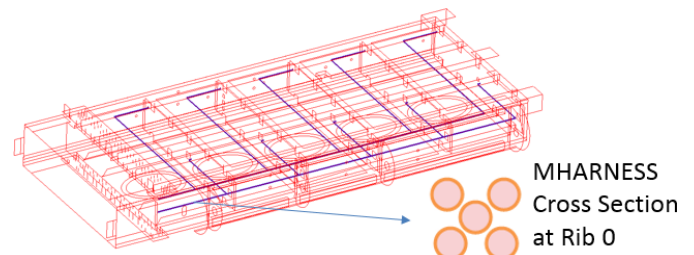


Figure 8: Layout and cross sectional view of harness bundles within the wing test box.

4.7 Simulation Speedup Techniques

All simulations were completed using parallel processing to greatly speed up computation time. Another speedup technique applicable to quasi-magnetostatic problems such as lightning was utilized. The magnetostatic time step (or gradual permittivity scaling formalism) is a standard feature of EMA3D [7] that can increase the permittivity throughout the problem space once the higher frequency content of the lightning pulse has exhausted; thereby allowing an increased time stepping for the problem. Increasing the FDTD step time can greatly reduce the total number of steps needed to complete a simulation.

5 Results Comparisons

The simulation techniques and engineering approximations described above for the CEM models are validated by comparing simulation results to experimental data for the wing test box. As mentioned in section 4.3, two models were used for numerical analysis to understand the results impact

of not resolving all anisotropies. The first model uses anisotropic material representation for the CFRP and ECF components and is called the anisotropic model. The second model that uses an isotropic material property for the bulk representation of CFRP and ECF is called the isotropic model. The isotropic model parameters in this effort were selected as high end estimates of the actual panel resistivities in an attempt to simulate worst case values for voltages and currents inside of the test box.

IEEE standard 1597.1 exists to validate CEM simulation results to experimental data using frequency domain comparisons and a feature selective validation (FSV) approach [8]. The authors found it difficult to apply this method to the transient phenomena of lightning. The limitations of the IEEE standard applicability to transient EMC problems have been established [9, 10]. An appealing alternative approach based on the FSV method but using comparisons in the time domain has been proposed [11], but time did not warrant a validation investigation using this proposed technique. Instead, a correlation between experimental and simulated of the wing test box was completed using peak value and action integral comparisons, which the FSV method is based on.

Scatter plots showing data points and margin lines can be used to observe an overall comparison quality. Figure 9 summarizes the comparison of currents and Figure 10 summarizes the comparison of voltages for simulated results and experimental data for all wing test box configurations. The data points are for a particular probe location and plot the simulated value against the experimental value. The red lines in the scatter plots illustrate where simulation and experimental results would be equivalent. The summary plots provide ± 6 dB variance lines which can be used to help establish margins for numerical simulation results. Data for both the anisotropic and isotropic models are presented in the scatter plots to illustrate the ability of the bulk isotropic model to accurately represent anisotropic materials. All of the results were normalized to a peak injection value of 20 kA.

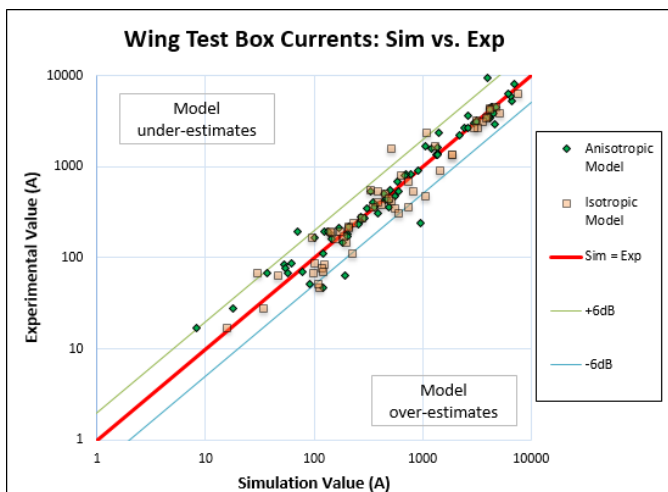


Figure 9: Validation summary of peak currents for anisotropic and isotropic models.

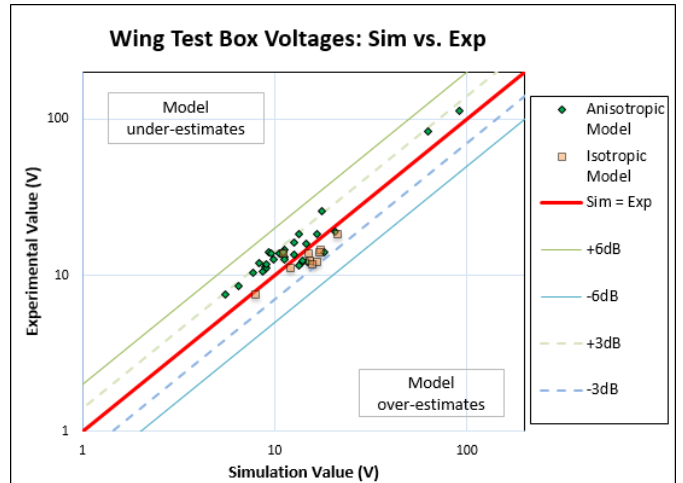


Figure 10: Validation summary of peak voltages for anisotropic and isotropic models.

An excellent correlation of simulation and experimental values is observed for a majority of probes, where more than 80% of the simulated current and voltage peak value results are within 3 dB of the experimental counterpart. Nearly 95% of all simulation probe values were within 6 dB of the experimental values.

Some sample waveforms are provided to show the types of comparisons made. These samples were chosen to illustrate the ability of the models and simulation techniques to not only capture exterior current distributions, but internal currents that are highly sensitive to the resistances of materials and connecting joints. Figure 11 shows a section of rib current that was measured near a fastener strike location. This probe was positioned a few cells down from the top level of the rib, where current distribution inside of a closed region can be difficult to capture without considering the impact of all fastener resistances.

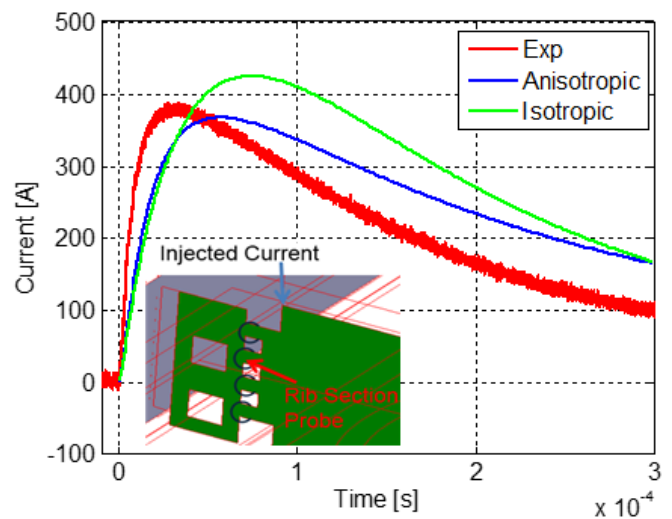


Figure 11: Comparison of a rib section current near injection point.

Figure 12 shows the CEM results comparison to an internal wire current measurement. Excellent agreement in peak amplitude and wave shape is observed between both models and the experimental result. For composite skinned aircraft, it is well established that electrical wiring can experience late time transient peaks around 100 μ s for Component A waveform strike. The lightning redistribution effect indicates that the aircraft current distribution is initially dominated by the inductive characteristics of the struck object, but then transitions to a resistively dominated response at later times [12]. Since the internal wires are shielded from the external environment by the structures they do not have peak times comparable to the injected waveform. Instead, these wires have resistances lower than those of the CFRP skins and spars and they tend to carry a larger portion of the injected current at later times when the current distribution is dominated by resistance.

The wire measured in Figure 12 spans multiple rib bays and crosses the wing test box from the forward to aft direction. Many parallel or alternative current paths exist in the test box from the beginning and ending termination locations of this wire. The peak experimental value of 200 A is 1% of the injected 20 kA, although the injected current value around 100 μ s is significantly less. The difference of the experimental data and both simulated results is less than 2 dB (15%). This is an astonishing correlation considering the complexity of the test box article and the small probed value relative to the injected waveform. Similar comparisons are observed for all internal wire currents.

The legend of Figure 12 indicates “Exp” which is the experimentally measured value, “Anisotropic” which is simulation model using anisotropic material properties for the test box skins and “Isotropic” which is the result for the simulation model when using isotropic material properties for test box skins. The same labelling approach is used for all of the remaining wave form plots.

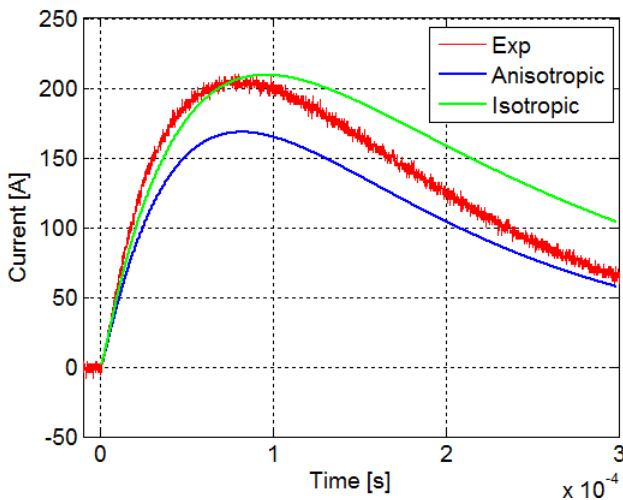


Figure 12: Comparison of experimental and simulation results on an internal wire current that spans multiple rib bays.

A small section of the exposed trailing edge CFRP spar was probed in Figure 13. This spar is on the exterior of the box making it an attractive path for the inductively dominated portion of the lightning pulse, illustrated by the high currents in the first few microseconds of the response. However, the current quickly changes paths away from this component because of the high resistivity of the bare CFRP spar compared to ECF covered panels and metallic TE strap. Again, both simulation models accurately capture both the inductive and resistive characteristic responses of the test box article to the lightning strike.

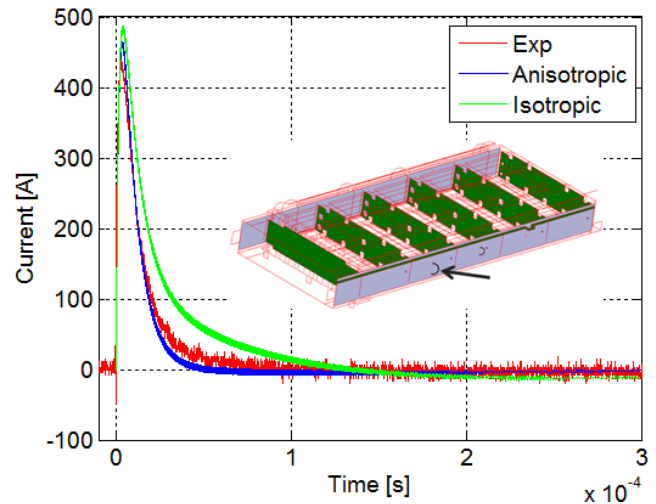


Figure 13: Comparison of experimental and simulation results on an exposed CFRP spar section.

All of the voltages measured on the wires within the test box article were obtained by connecting the internal wires to a rib at one end, leaving the wire open at the other end and measuring the voltage between the open wire and root rib. A simple moving average algorithm is applied to the simulation data. Figure 14 shows a wire voltage for a fastener injection case with an excellent overall agreement between both simulation models and the experimental result.

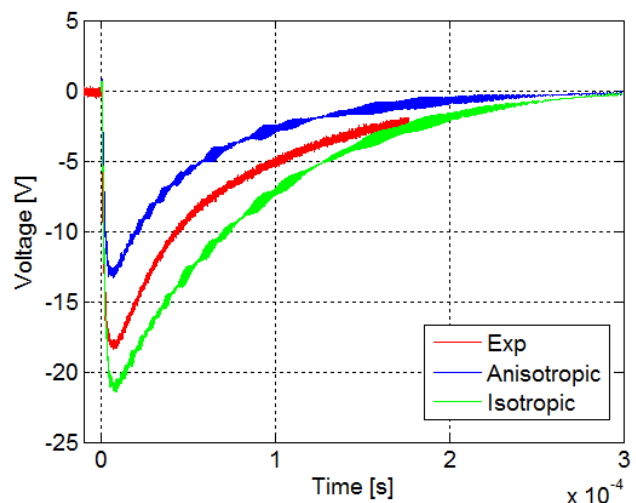


Figure 14: Comparison of experimental and simulation results for an internal wire voltage to a rib.

6 Conclusions

CEM simulations using EMA3D can be used to support a certification program and to evaluate the lightning response of a complex aircraft system. When using simulations in the certification process it is important to have experimentally validated models and analysis techniques. Analyzing a wing test box can be an essential step between panel testing and full aircraft testing because it allows the study of complex connections between skins, spars, ribs and system like components without the complexities of testing a full scale aircraft. The validation of simulation techniques can also be achieved more simply for test box articles.

It is not possible to resolve all features of complex aircraft designs and approximations must be developed in the modeling approach. Certain features of the model, including accurate panel conductivities and contact resistance of fasteners to different material types, are critical to capture accurate current distributions and developed potentials for the wing test box response to lightning current injections.

A significant portion of the wing test box simulation results and experimental data comparisons, 80% of the 100+ total probes, are within a 3 dB peak value range. The current and voltage comparisons for both models, isotropic and anisotropic, are excellent across all external and internal measurements. Figures 12-14 illustrate how isotropic surface material parameters in a simulation model can be selected to generate conservative results for currents and voltages inside of enclosed test box. The simulation approach and modelling techniques described in this validation effort lend confidence that CEM simulations, with or without anisotropic material representation, can accurately capture the complex lightning response of aircraft built with CFRP materials.

7 Acknowledgements

All of the authors deserve significant recognition for their contributions and input to this effort. The collaborative venture of Bombardier and EMA has been cooperative and enlightening. The wing box tests were conducted by the technical staff from NTS Lightning Technologies at their facility in Pittsfield, MA. The EMA staff completed many of the material property measurements at their facility in Lakewood, CO.

8 References

- [1] Wahlgren, Bo. I., and Rosen, Jonas W.: 'Finite Difference Analysis of External and Internal Lightning Response of the JAS39 CFC Wing'. International Aerospace and Ground Conference on Lightning and Static Electricity, Oklahoma City, USA, April 1988, pp. 396-400
- [2] Satake, K., Yamamoto, S., Yamakoshi, H., Aoi, T. Iyomasa, A. and Murakami, K.: "Development of Electromagnetic Simulation Supporting Lightning Protection Design of Mitsubishi Regional Jet", *Mitsubishi Heavy Industries Technical Review*, vol. 49, no. 4, 2012, pp. 79-84
- [3] SAE ARP5415 Rev. A: 'User's Manual for Certification of Aircraft Electrical/Electronic Systems for the Indirect Effects of Lightning', 2002
- [4] SAE ARP5416: 'Aircraft Lightning Test Methods', 2005
- [5] SAE ARP5412: 'Aircraft Lightning Environment and Related Test Waveforms', 1999
- [6] Kitaygorsky, J., Elliott, J. R., Kamihara, N., Satake, K. and Yamamoto, K.: "Modeling the effects of anisotropic material properties on lightning-induced current flow in structures containing carbon fiber reinforced plastic," *ICOLSE 2009 Conference Proceedings, 2009*, pp. 15-17
- [7] Rigden, G.: "Manual #5 - EMA3D Preparation Manual," June 2014
- [8] IEEE 1597.1: 'IEEE Standard for Validation of Computational Electromagnetics Computer Modeling and Simulations', 2008
- [9] Telleria, R., Silva, F., Orlandi, A., Sasse, H., Duffy, A.: "Factors influencing the successful validation of transient phenomenon modelling," *Asia-Pacific International Symposium on Electromagnetic Compatibility, Beijing, China, April 2010*, pp. 338-341
- [10] Jauregui, R., Rojas-Mora, J., Silva, F.: "Study of Transient Phenomena with Feature Selective Validation Method," *Progress In Electromagnetics Research Symposium Proceedings, Marrakesh, Morocco, March 2011*, pp. 1113-1117
- [11] Jauregui, R., Riu, P., Silva, F.: "Transient FDTD Simulation Validation" *IEEE Proceedings 2010*, pp. 257-261
- [12] Fisher, F. A., Plumer, J. A., Perala, R. A.: "Lightning Protection of Aircraft", *Lightning Technologies, Inc.*, 1990, pp. 316-323